

Proficiency of Graphene Oxide in Adsorption of Zn(II) Ions from Aqueous Solution

N.A. Udoka* and E.C. Kenekwukwu

Department of Chemistry, Federal University of Technology Owerri, P.M.B. 1526, Owerri, Nigeria

(Received 1 September 2018, Accepted 12 December 2018)

The efficient adsorption of metals on graphene oxide is often affected by the preparation method. Graphene oxide was prepared using a typical modified Hummers method for adsorptive removal of Zn^{2+} from aqueous solution. The experimental data were fitted into the Langmuir isotherm. The reaction was irreversible, but had a small energy of adsorption which was indicated by Freundlich isotherm model. Tempkin model and Dubinin Radushkevich revealed a physical adsorption process driven by a slow adsorptive process. The Pseudo 2nd order had the best correlation coefficient at 0.9958 while Langmuir was 0.9545. Elovich function indicated a non-spontaneous reaction, while the intra-particle diffusion was not the rate-determining step. The slow adsorption rate in pseudo 1st order correlated with the small adsorption energy shown by the Freundlich isotherm, and also correlated with the small boundary layer thickness shown by intra-particle diffusion. All adsorptive functions showed that some other competing mechanisms should exist. XRD showed an increased number of graphene layers, d-spacing and improved crystallite size. FTIR data showed the oxygen-containing groups on the graphene oxide surface. The study showed that the prepared graphene oxide could efficiently adsorb Zn^{2+} , and that the adsorption is affected by the method of synthesis.

Keywords: Graphene, Graphene oxide, Adsorption, Zinc ions

INTRODUCTION

Graphene and graphene oxide (GO) derivatives have shown superiority in adsorption studies due to their unique surface properties (functional groups) and functionalization potentials [1,2,3].

During preparation and synthesis, GO can be exfoliated both mechanically and chemically into several layers. However, the size and method of synthesis for precursor materials are important determinants in adsorption applications [4]. The chemistry and reactivity of GO delivers several potential possibilities for improved mechanical, electrical, thermal and adsorption materials applications during and after synthesis [3,5].

Literature review of graphene and its derivatives showed that enhanced improvement in GO tuneable large surface area, including several hydrophilic layers and basal planes,

can be achieved through synthesis; hence a passable material for adsorption studies [6,7]. Similarly, the tenability of the functional groups on the surfaces of GO such as carbonyl, epoxy and hydroxyl, improves its adsorption ability over adsorbates as well as compatibility with other materials [8,9]. Moreover, GO makes nucleation sites for the growth of inorganic materials [10]. The Hummers method has remained a safe and easy preparation route due to the removal of powerful oxidizing agents [11]. Modified hummers method however, makes use of extra amounts of H_2SO_4 , $NaNO_3$ and $KMnO_4$ which reduces destruction of reactive sites, whereas Brodie's method uses HNO_3 and $KClO_3$ [12,13,14].

Although many preparation routes are being explored, scale up and low yield has remained a problem as noted by [15]. As a result, precursors like petroleum pitch based carbon fibre has been developed [16]. Using cross flow filtration and cell dialysis, researchers have purified GO materials and reported scale-up to 60 g and 120 g [17,18]. In

*Corresponding author. E-mail: chemistryfrontiers@gmail.com

addition, microwave assisted method used by [19], and GO preparations used by [20,21] showed that basal planes were improved; hence suitable for higher yield and low toxic emissions. Thus, research has continued to improve GO adsorption applications using nano-carbon sorbents for removal of heavy metals such as Cu^{2+} , Co^{2+} , Cd^{2+} , Zn^{2+} , Ni^{2+} and Pb^{2+} metals during water treatments [22] well as, the removal of synthetic organic compounds like phenanthrene and biphenyl in waste water treatment [23]. In addition, GO has been used for adsorption of trace and ultra-trace rare earths in tea leave elements using solid phase extraction procedure by [24]. Also, synthesized 3D functionalized graphene hybrid electrodes concurrently detected heavy metals Pb^{2+} and Cd^{2+} in anodic stripping voltammetry of effluent samples with several active surface contamination as experimented by [25].

Studies by [26] showed that functionalized graphene oxide can adsorb Zn^{2+} in aqueous solvents, while carbon nanotube was applied for Zn^{2+} adsorption in studies performed by [27]. In this respect, our previously reported experiment showed that kinetic adsorption studies of Zn^{2+} removal by GO in aqueous solution is easily modelled and gives a good isotherm fitting [28]. Albeit, the authors used different GO preparation methods, and they reported different adsorption results. Their distinct findings showed that sorption properties of GO depend on pH, ionic strength, temperature and nature of functional groups generated during synthesis. Hence, the application of GO to efficiently remove Zn^{2+} in aqueous solution depends on the method of preparation. The study will therefore, investigate the proficient adsorption capability of GO over Zn^{2+} in aqueous solution, using atypical modified Hummers method (Hou *et al.* 2013; Paulchamy, Arthi and Lignesh, 2015).

MATERIALS AND METHODS

Materials

All reagents of graphite powder, H_2SO_4 , KMnO_4 , H_2O_2 , HCl and NaOH, purchased from Fisher Scientific, were of analytical grade with 97-98% purity. The aqueous solutions were prepared with double-distilled water (DDW) taken from Physics Laboratory of Federal University Owerri. All experiments were carried out using 500 ml and 1000 ml

conical flask and pyramid glass bottle. Atomic absorption spectroscopy model AA 500 Pg and X-ray diffraction analysis (XRD) Equinox 300 model and Fourier transform infrared Spectroscopy (FTIR) of Perkin Elmer 8790 model instruments were used to determine the concentrations of heavy metals in the supernatant liquids and morphological properties. The solutions were diluted with 0.1 M NaOH or 0.1 M HCl as required. All experiments were run in triplicates and average values were reported.

Preparation of Graphene Oxide

4 g of graphite powder was weighed into a 1000 ml volumetric flask. 180 ml of H_2SO_4 was added to the solution and kept under continuous stirring between 0-5 °C using an ice bath. The solution was stirred at this temperature for 5 h. 24 g of KMnO_4 was added slowly within 5 min and the reaction temperature maintained at 10-15 °C. About 370 ml of water was added gradually with continuous stirring while gently decreasing the reaction temperature to stabilize at 35 °C. Using reflux system, the mixture was refluxed in series as follows: 30 min at 98 °C, 20 min at 40 °C, and 20 min at 20 °C with notable brown colouration and allowed to equilibrate for 2 h at 20 °C. Then, 80 ml of H_2O_2 was introduced over a period of 5 min which caused equivalent bright yellow appearance. The solution was further diluted with 400 ml of water and 10% HCl, and afterwards, centrifuged for 5000 rpm at 10 min. The obtained mixture was filtered and washed to neutral pH 7 using deionized water. The black gelatine substance was dried at 80 °C for 4 h to get the graphene oxide powder (Paulchamy, Arthi and Lignesh, 2015).

Adsorption of Zinc

20 mg of GO was weighed into 20 ml of Zn^{2+} solution with a known initial concentration of 15 mg l^{-1} . The mixture was stirred using a magnetic stirrer for 20 min at 30 °C and then centrifuged for 60 min at 10,000 rpm. The pH was kept constant at 7 and reaction mixture kept between 28 -30 °C. After 60 mins, the GO was filtered, and the filtrate was analysed using AAS to determine the amount of Zn^{2+} in the filtrate. Adsorption capacity q (mg g^{-1}) was further obtained according to Eq. (1) (Nkwoada, Okoli and Ekeanyanwu, 2016; Najafi, 2015),

$$q = [(C_0 - C_f) \frac{V}{M}] \quad (1)$$

where C_0 and C_f are the initial and final concentrations (mg l^{-1}) of Zn^{2+} ions in the aqueous solution, respectively. M is the mass of adsorbent and V is the volume of Zn^{2+} ion solution.

Batch adsorption studies of Zn^{2+} . Batch adsorption of Zn^{2+} over the adsorbent GO was carried out in a 250 ml airtight conical flask. The flask contained 20 ml of a known concentration (15 mg l^{-1}) of the solution and an accurately weighed amount of the adsorbent. The mixtures in the flask were agitated on a magnetic shaker for 10 min and operated at a constant speed of 150 rpm. The mixture was centrifuged at 10,000 rpm at 30°C and at pH 7. The effect of contact time were (10, 20, 40, 60, 80, 120, 150, 180 min), and adsorbent dosages (10, 20, 30, 40, 50, 60, 80, 100 mg) were tested. The flask containing the samples were withdrawn from the shaker at the predetermined time intervals, filtered and final concentrations of Zn^{2+} in the supernatant solutions were determined using AAS. The Zn(II) ion adsorption capacity at time t (q_t), in mg g^{-1} , was calculated using Eq. (2) described by [29] and [26],

$$q_t = [(C_0 - C_t) \times \frac{V}{M}] \quad (2)$$

where C_0 (mg l^{-1}) is the initial Zn(II) ion concentration, C_t (mg l^{-1}) is the Zn(II) ion concentration at time t , W (g) is the adsorbent mass, and V (l) is the volume of Zn(II) ion solution.

Adsorption Isotherms

Heavy metals, adsorbed *via* solid adsorbent through an adsorption process, attains equilibrium when the concentrations of such adsorbates in solution and in water are constant. Then, equilibrium relationship of that interaction gives the adsorption isotherm. The Langmuir isotherm model assumes a uniform energy of adsorption at a constant temperature on a single layer of adsorbed solute. The linear form is expressed in Eq. (3) [22],

$$\frac{C_e}{q_e} = \frac{1}{qmKl} + \frac{C_e}{q_e} \quad (3)$$

where q_e (mg g^{-1}) is the amount of zinc ions adsorbed at equilibrium, C_e is the equilibrium zinc ion concentration (mg l^{-1}) and Kl is Langmuir constant related to the binding strength of zinc ions onto the graphene oxide. Langmuir isotherm separator factor is expressed in terms of the parameter RL . It is a dimensionless constant. The value of RL shows the significance of the reaction. If $RL > 1$, it is unfavourable, if $RL = 1$, it is linear, if $0 < RL < 1$ it is favourable, and it is irreversible if $RL = 0$.

The Freundlich isotherm is used for describing solute distribution between aqueous and solid phases. It assumes an exponential site variation in adsorbent energies giving the fall in heat as a function of logarithm. Freundlich is also an empirical equation and expressed as (Wang *et al.* 2012):

$$\log q_e = \log Kf + \frac{1}{n} \log C_e \quad (4)$$

The Freundlich constant Kf represents the adsorption capacity ($\text{mg}^{1-n} \text{l}^n \text{g}^{-1}$) while n is the strength (energy) of the adsorption. The q_e is known as the loading adsorbate on the adsorbent, attained at equilibrium (mg g^{-1}).

Temkin isotherm makes the assumption that heat of adsorption of all molecules in the layer would linearly decrease with exposure, hence owing to the adsorbate interactions instead of logarithmic but ignoring the very high and low concentrations. The linearized form is given as Eq. (5) [30].

$$q_e = B \ln KT + B \ln C_e \quad (5)$$

KT (M) represents the equilibrium binding constant corresponding to the maximum energy binding energy. B refers to the constant related to the heat of adsorption and the differential surface capacity for the zinc sorption capacity per unit binding energy. If the value is less than 8 KJ mol^{-1} , then there is a weak interaction between the adsorbate and adsorbent, indicating a physical adsorption.

The Dubinin-Radushkevich (DB) isotherm model is used for expressing heterogeneous surface adsorption mechanism using Gaussian energy distribution. It normally fits into surfaces with high solute activities and intermediate concentrations and often expressed linearly as shown in Eq.

(6) (Dada, Olalekan, Olatunya and Dada, 2012).

$$\ln q_e = \ln q_s - \beta \varepsilon^2 \quad (6)$$

The β represents a constant, relating to the mean free energy of adsorption per mole of the dye ($\text{mol}^2 \text{kJ}^{-2}$) and transferred to the surface of the adsorbent from infinity in solution, q_s represents the theoretical saturation capacity, and ε stands for the Polanyi potential governing the reaction and expressed as shown in Eq. (7),

$$\varepsilon = RT \ln(1 + 1/C_e) \quad (7)$$

where R, T, and C_e represents the gas constant (R), absolute temperature (K), and adsorbate equilibrium concentration (mg l^{-1}). The DB isotherm is temperature dependent, and when the temperatures are plotted as a logarithm function against the squared potential energy, it produces a unique curve such that the points lie in plain.

Kinetic Isotherm

Different adsorption kinetic isotherms have been employed to describe adsorption processes. We used pseudo-first-order, pseudo-second-order, power function and intra-particle to describe the sorption kinetics of Zn^{2+} over graphene oxide.

The pseudo-first-order is commonly applied for solid/liquid adsorbent system. The Lagergren's pseudo-first-order equation is expressed in linear form as

$$\ln(q_e - q_t) = \ln q_e - K_1 t \quad (8)$$

q_e and q_t are the concentration of metal ions adsorbed per gram of the adsorbents (mg g^{-1}) at equilibrium and at time t (min). K_1 is the pseudo-first-order adsorption rate constant (min^{-1}). A plot of $\ln(q_e - q_t)$ would give a straight line from which the slope and intercept can be calculated [26].

The pseudo-second-order is stated below

$$\frac{t}{q_t} = \frac{1}{K_2 q_e^2} + \frac{t}{q_e} \quad (9)$$

A plot of t/q_t vs. t gives a linear relationship that allows the computation of K, h and q_e constants. K is the pseudo-

second order adsorption rate constant ($\text{g mg}^{-1} \text{min}^{-1}$) and q_e is the amount of the Zn^{2+} ion adsorbed (mg g^{-1}) over GO at equilibrium. Its initial sorption rate, h ($\text{g mg}^{-1} \text{min}^{-1}$) is expressed as $h = K q_e^2$. The agreement between the experimental and calculated value of q_e gives the applicability of the model.

The intra-particle diffusion is used for description of sorption processes in solid-liquid systems. The sorption is characterized by mass transfer of solute from the solution to the adsorbents particle surface, the uptake of the adsorbate at the binding site and the intra-particle diffusion. The Weber and Morris equation is often employed because the batch process being controlled by the sorption rate parameters provides high possibility for occurrence of pore diffusion (Abuh, *et al.* 2013). The equation is expressed as given in Eq. (10).

$$Q_t = K_i t^{1/2} + C \quad (10)$$

The plot of q_t vs. $t^{1/2}$ gives a straight line graph where C is the intercept representing the effect of the boundary layer thickness, and K_i is the intra-particle diffusion rate constant ($\text{mg g}^{-1} \text{min}^{1/2}$). If the line passes through the origin, then intra-particle diffusion is the main rate-controlling step in the adsorption process, but if it appears as multi linear plots then some other adsorption processes have influenced the system.

The Elovich function was used to investigate the mechanism of adsorption of Zn^{2+} over the graphene oxide. Although widely accepted, it predicts the kinetics of chemisorption of gases onto solids, however, it does not provides any definite mechanism for adsorbate-adsorbent interaction. The linear form is expressed by Eq. (11).

$$q_t = \frac{\ln(\beta\alpha)}{\beta} - \frac{\ln t}{\beta} \quad (11)$$

The α and β constants are the initial adsorption rate ($\text{mg g}^{-1} \text{min}^{-1}$) and desorption constant ($\text{g mg}^{-1} \text{min}^{-1}$) during the experiment, respectively. A plot of qt vs. $\ln t$ gives a slope with $1/\beta$ value which is indicative of the number of sites available for adsorption (Abuh *et al.* 2013).

RESULTS AND DISCUSSION

Material Characterization

The XRD pattern is a technique used for morphological study of materials like graphite, graphene and graphene oxide. It determines the spacing between the layers and orientation of the studied atoms of a single crystal or grain. The determined pattern for the graphene oxide and graphite is shown in Fig. 1, also with the full width at half maximum (FWHM) graph evaluated from the plot using Origin 9.0. It was found that peak of 25 degrees was found for graphite which shows a high level of arrangement and interlayer distance of 3.55 Å along the (002) orientation. The appearance of the graphene oxide peak at 12 degree evidences that the prepared GO has been oxidized and may be exfoliated. Therefore, the increase of d spacing to 7.37 Å and improved for adsorption due to presence of oxygen rich functional groups (Paulchamy, Arthi, & Lignesh, 2015). The interplanar distances were determined using Bragg's equation of $n\lambda = 2d\sin\theta$. Wherein n is assumed to be 1, λ represents the wavelength of X-ray source (1.541 Å) and θ is half of the corresponding angles in radians. The Debye-Scherrer equation was used to determine the particle size of samples or average crystallite width (D), given as $D = k\lambda/\beta\cos\theta$. In which λ is X-ray wavelength (1.541 Å), D represents the average crystallite size, β is line broadening in radians, θ is Bragg's angle, and k is Scherrer's constant (0.9). The calculated crystallite size determined for graphite was 1.22 nm while graphene oxide showed an increase in size at 3.27 nm. The crystallite size showed that the graphite contained some lateral defects and reduced in graphene oxide. The above result was relatively similar to crystallite sizes obtained by [32] but differs from [33]. Hence, the synthesis of graphene oxide affects the nature of lateral defects induced and graphene layers developed. In addition, the combination of Debye-Scherrer and Bragg's equations gives an expression for n which represents the number of graphene layers per domain. This gives an approximate value of n from XRD peak broadening. The calculated graphene layer (n) for graphite was (n = 2) and graphene oxide was (n = 5). According to Sharma, Chadha and Saini, (2017) the consequent layer packing in GO is due to various oxygen functional groups causing strong molecular

attraction, while fewer oxygen functional groups exist in graphite with consequent diminishing molecular attraction [32].

The FTIR spectrum in Fig. 2 shows the functional groups on the surface of GO. The different peaks were 3438 cm^{-1} (O-H stretching), 1711 cm^{-1} (C=O), 1624 cm^{-1} (C=C), 1420 cm^{-1} (carboxyl C-O) and 1230 cm^{-1} (epoxy C-O) stretching. They showed that the GO surface was rich in oxygen-containing functional groups which was correlated with XRD findings [22,26].

Effect of Contact Time

In the study of the adsorption process, contact time is a very useful parameter. Figure 3 shows the effect of contact time on the removal of Zn^{2+} by graphene oxide. The results showed that the adsorption capacity increased with increasing contact time. The experiment was conducted from 10 to 180 min. It was observed that the synthesized graphene oxide attained equilibrium at 90 min with a capacity of 0.52 mg g^{-1} . However, [27] had reported maximum saturation of their synthesized single walled and multi-walled soluble carbon nanotube at 60 min while [26] reported 40 min as the contact time for both graphene oxide and functionalized graphene oxide to reach equilibrium. Also experiment conducted by [29] showed that maximum saturation was around 120 min for adsorption of Zn^{2+} by graphene oxide. Hence, large vacant adsorption sites may be suggested to be present in the prepared graphene oxide.

Effect of Adsorbent Dosage

The effect of adsorbent dosage is also shown in Fig. 3. The experiment was conducted from 10 to 100 mg. Observation showed that the overall removal efficiency is decreased as the adsorbent dosage increases. This decrease may be due to the corresponding non availability of adsorption sites. Also, observation showed a sharp decrease at 80 mg and appeared saturated at 100 mg. Thus, it may be suggested that the amount of Zn(II) ions adsorbed per unit mass after 100 mg becomes unaffected by the dosage amount. [29] experimental data, similar had a sharp decrease, followed by an increase and saturation (maximum dosage amount). However, the prepared graphene oxide has shown higher adsorption at smaller dosages than at large

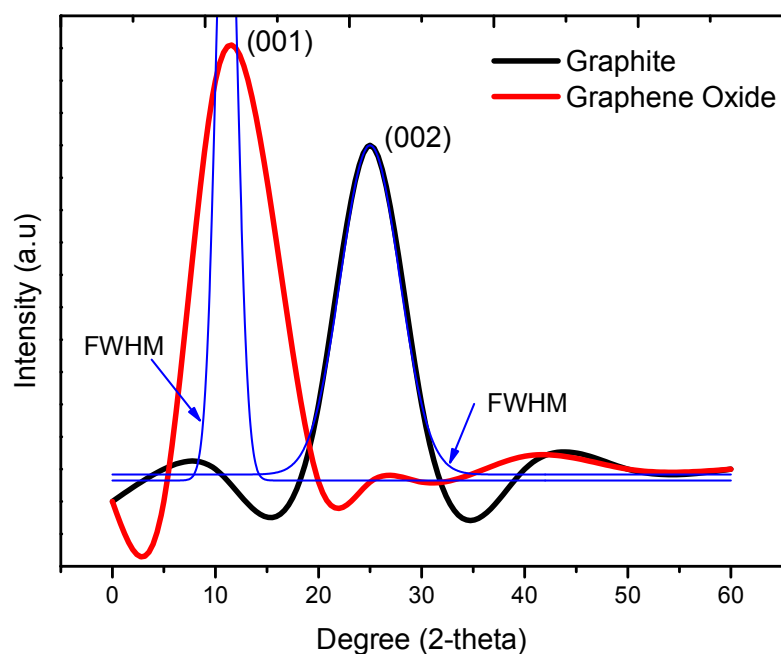


Fig. 1. Graphene oxide and graphite XRD patterns.

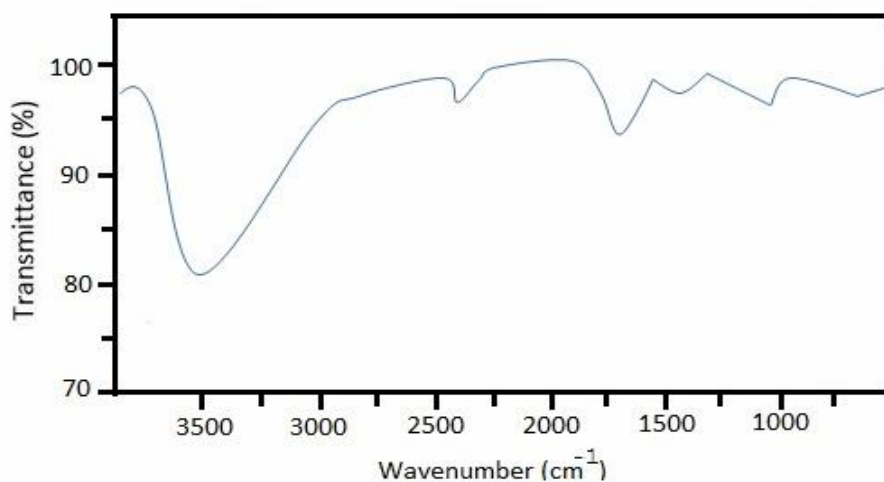


Fig. 2. FTIR spectrum of graphene oxide.

dosage/amount. Smaller dosage amount may have been energetically favourable due to diminutive obstruction of the basal planes by Zn^{2+} . This effect is because zinc ions are

known to induce the compacting of GO because of the strong interaction that exist between Zn^{2+} and carboxyl groups found in the graphene oxide.

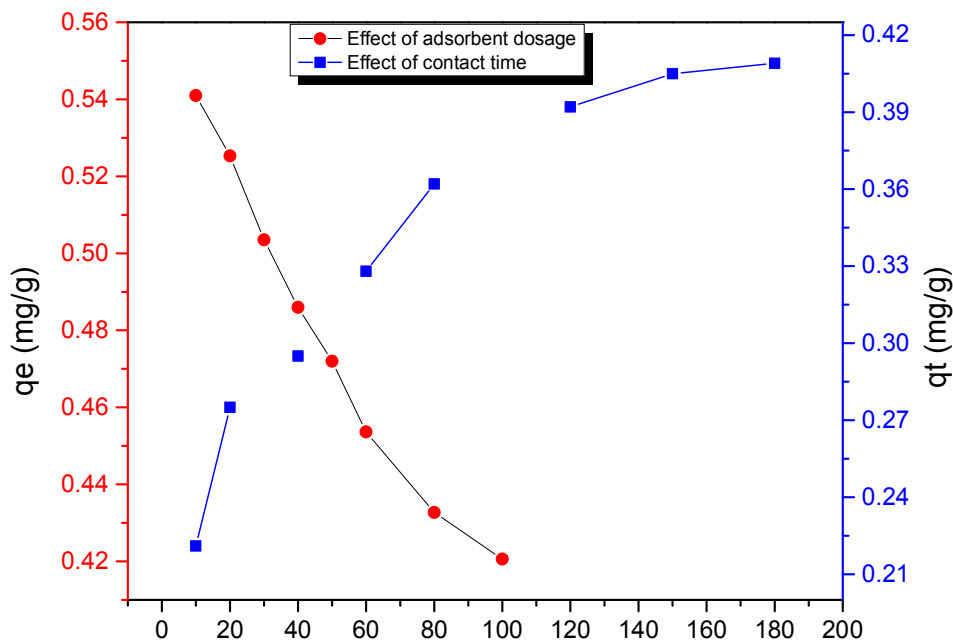


Fig. 3. Effect of contact time and adsorbent dosage.

Adsorption Isotherm

The adsorption isotherm graphs are shown in Fig. 4. The graphical inspection of the residual plots for Langmuir, Freundlich, Tempkin and Dubinin-Radushkevich showed no regular pattern or trend. Hence, a pointer to a good R^2 fitting. The correlation coefficient (R^2) of the four isotherm graphs were examined. The isotherms gave a good fitting regarding experimental data. However, with Freundlich at 0.9937 and Langmuir at 0.9545, both gave the best and least fitting among the four adsorption isotherm graphs. Also, observation showed that Langmuir and Dubinin Radushkevich had negative adsorptive interaction while Freundlich and Tempkin showed a positive interaction of both the X and Y axis. The values of the absolute slope and intercept are presented in Table 1. It revealed that Langmuir has a significantly larger intercept (57.3366) compared to others, suggesting rapid adsorption rates for the adsorbates. Their slopes were < 5 and showed negligible standard errors.

The Langmuir isotherm provided a poor fitting based on R^2 compared to the other three isotherm functions. Similarly, such poor fitting of zinc ions using Langmuir isotherm onto graphite oxide was also reported by [34]. The

K_L is the binding constant and had a value of 28.1006. These showed that the binding strength of the zinc ions onto the graphene oxide was larger enough to cause a higher value of the intercept. Hence, the higher the K_L value, the higher the intercept regarding Langmuir isotherm. The high binding energy obtained through computational studies of divalent ions by [35] showed that Zn^{2+} has two positions on the graphene oxide sheet after optimization and, therefore, has a higher binding energy.

Interestingly, R_L was 0.0023 and confirmed that the reaction was favourable. Also [26] synthesized graphene oxide and used Langmuir type 1 to evaluate the results, which showed similar R^2 value of 0.9592, wherein R_L less than 1 showed favourable reaction. The amount of adsorbate on the adsorbent at equilibrium is indicated by q_m as shown in Table 1, indicating that Zn^{2+} remained will be very small when equilibrium is attained, as also see in Fig. 3.

The Freundlich gave the best fitting correlation coefficient value. This correlated with the high value of K_F (96.0505) which confirmed the sensitivity adsorption capacity of the graphene oxide and the Freundlich function to identify such relationship. The strength/energy (n) of the adsorption process was small at 1.9665, indicating a slow

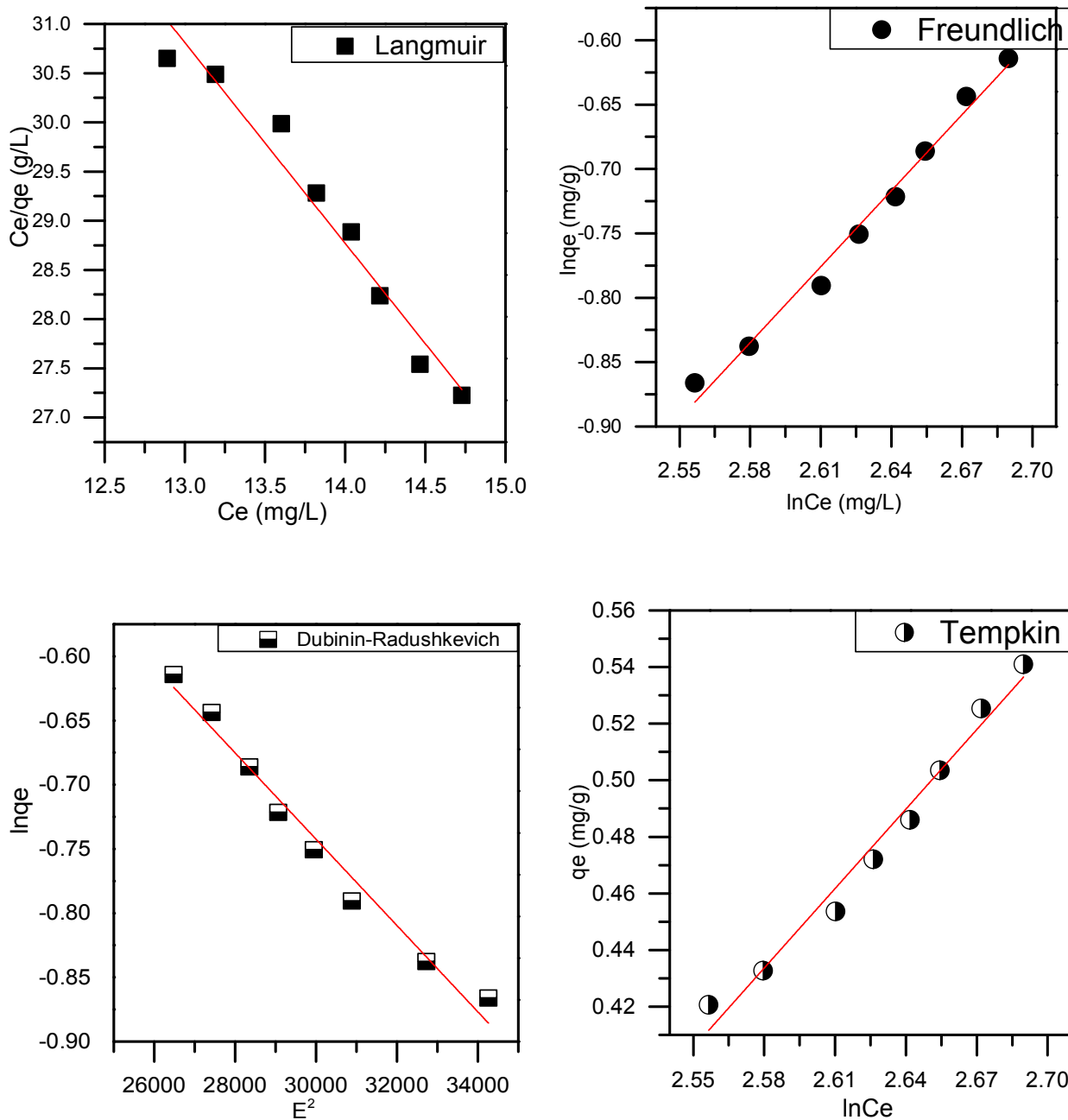


Fig. 4. (L-R) Adsorption isotherm graphs for Zn^{2+} adsorption by GO showing Langmuir, Freundlich, Dubinin-Radushkevich and Tempkin isotherms.

adsorption mechanism. Hence, rapid adsorption may be observed if heat is added to the system to increase the energy required for migration of the zinc ions.

The Dubinin Radushkevich also produced a good fitting

correlation coefficient. Based on its description, there was a high solute activity and a heterogeneous surface adsorption mechanism occurring in-between Zn^{2+} and GO. β representing the mean free energy was very small and

Table 1. Graphical Parameters and Calculated Values from Adsorption Isotherm Graphs

	R ²	Slope	Intercept					
Langmuir	0.9545	2.0404	57.3366	q _m (mg g ⁻¹)	0.0174	K _L (l mg ⁻¹)	28.1006	R _L 0.0023
Freundlich	0.9937	1.9665	5.9086	K _F (mg g ⁻¹) (l mg ⁻¹) ^{1/n}	96.0505	n	0.9665	1/n 1.0346
Dubinin- Radushkevich	0.9755	3.36 × 10 ⁻⁵	0.2656	β (mol ² kJ ⁻²)	3.36 × 10 ⁻⁵	Q _s (mg g ⁻¹)	1.3042	
Temkin	0.9768	1.9825	0.9365	β (kJ mol ⁻¹)	1.9825	K _T	1.6038	

Table 2. Graphical Parameters and Calculated Values from Adsorption Kinetic Graphs

	R ²	Slope	Intercept					
Pseudo 1 st	0.9723	0.0185	0.8470	Q _e (exp) (mg g ⁻¹)	0.0721	K ₁ (g mg ⁻¹ min ⁻¹)	0.0426	q _e (cal) (mg g ⁻¹) 7.0307
Pseudo 2 nd	0.9958	2.2683	34.6211	H (mg g ⁻¹ min ⁻¹)	0.0288	K ₂ (g mg ⁻¹ min ⁻¹)	0.1486	Q _e (cal) (mg g ⁻¹) 0.4408
Elovich	0.9789	0.0667	0.0650	B (g min ⁻¹)	0.0667	α (mg g min ⁻¹)	0.1767	1/β 14.9925
Intra particle diffusion	0.9567	0.0182	0.1825	K _{id} (mg g ⁻¹ min ⁻¹)	0.0182	C (mg g ⁻¹)	0.1825	

2013). This is due to the strong surface complexation of zinc ions with oxygen-containing functional groups that correlates with the large active site present on the GO surface which was also detected by Elovich function.

The H (mg g⁻¹ min⁻¹) value of the pseudo 2nd order which showed the initial adsorption rate of zinc(II) ions by GO was small (0.0288) regarding time. The adsorption rates constant, K₂, was 0.1486 (g mg⁻¹ min⁻¹) that showed a fast kinetics. However, the q_{e(cal)} term from pseudo 2nd order was 0.4408 while q_e determined from experiment was maximum at 0.5410 and a minimum at 0.4206 value. This shows the applicability of this kinetic function to evaluate the graphene adsorption of Zn²⁺, and similarly reported by [26,

29], the intercept was high compared to the other kinetic functions and agreed well with the correlation coefficient which was the best fit at 0.9958

The Elovich function predicts the kinetics of chemisorption of gases onto solids. The experimental data were fitted well into the Elovich function giving R² as 0.9789 and thus suggests chemisorption process as part of agreed with the n value of the Freundlich isotherm. Also, the theoretical saturation (q_s) was 1.3042. At such a small value, the theoretical saturation correctly predicted that equilibrium could be a slow and gradual process.

The Temkin isotherm similarly produced a good correlation coefficient fitting. The K_T term representing the

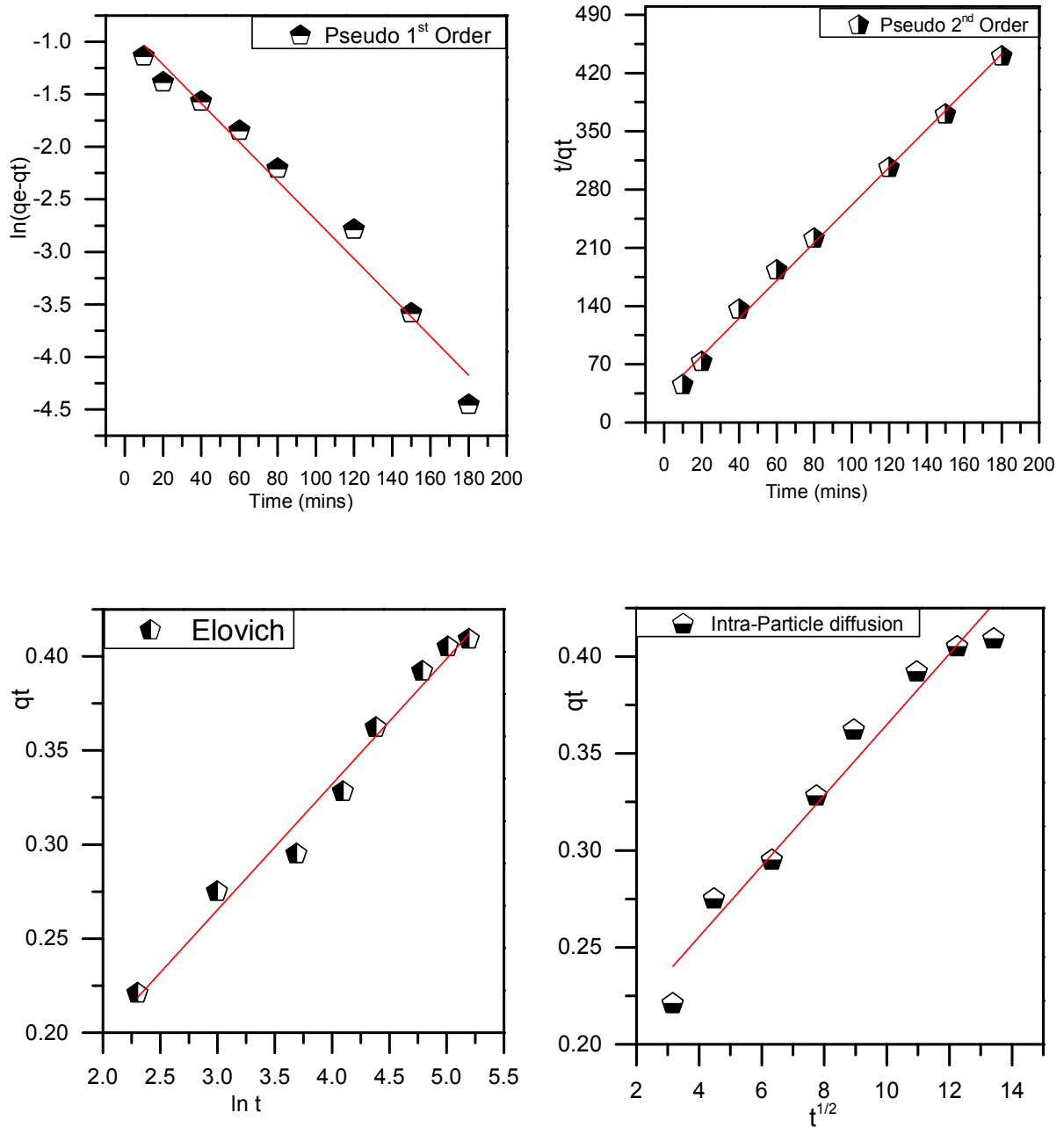


Fig. 5. (L-R) Adsorption kinetic graphs for Zn²⁺ adsorption by GO showing Pseudo 1st order, Pseudo 2nd order, Elovich and Intra particle diffusion.

equilibrium binding constant and the maximum energy was 1.6038, and the B term representing the heat of adsorption and sorption capacity per unit binding energy was 1.9825. Both parameters agreed with the theoretical

saturation (q_s) of Dubinin Radushkevich and the strength/energy of adsorption (n) in Freundlich. The low values of KT and B (less than 8 kJ mol⁻¹) were indicative of a weak binding interaction, and consequently a

physical adsorption process in the system. Therefore, the four adsorption isotherms have shown the proficiency of graphene oxide in the removal of zinc(II) ions in aqueous solution.

Adsorption Kinetics

The removal of heavy metals in aqueous solution regarding contact time is very crucial. Graphs of the adsorption kinetics plotted for pseudo 1st order, pseudo 2nd order, Elovich and Intra particle diffusion graphs are shown in Fig. 5. Residual plots inspected showed no trend or pattern, indicating a good correlation coefficient. R^2 of pseudo 2nd order gave the best line of fit at 0.9958 while the intra-particle diffusion gave a least fitting curve with R^2 at 0.9567. Graphical observation showed that the adsorption kinetics of pseudo 1st order decreased just as time increased, while the adsorption kinetics of Elovich, pseudo 2nd order and intra-particle diffusion increased just as time increased. Their slopes were lower than 5, indicating a negligible standard error.

The pseudo 1st order had $q_{e(cal)}$ larger than $q_{e(exp)}$. It shows that the concentration of the adsorbed metal ions in the experiment was much lower than the concentration of adsorbed metals obtained by calculation. The K_1 term representing the rate constant was $0.0426 \text{ (g mg}^{-1} \text{ min}^{-1})$ that signifies a small fraction of adsorption rate regarding time. Also, the slopes and intercepts, as seen in Table 2, had smaller absolute values which correlated with the rate constant value. Also, adsorption study of divalent behaviour of Zn ions in aqueous solution by graphene oxide shows that pseudo 1st order usually provides less favourable fitting in zinc adsorption compared to pseudo 2nd order [36], the adsorptive interaction. The initial adsorption rates and desorption constant (α and β) showed a small initial adsorption as seen in $H \text{ (mg g}^{-1} \text{ min}^{-1})$ of pseudo 2nd order and $K_1 \text{ (g mg}^{-1} \text{ min}^{-1})$ of pseudo 1st order. However, the desorption constant was low at 0.0667 indicating that the interaction between adsorbent and adsorbate was not spontaneous. Subsequently, the large value by $1/\beta$ at 14.9925 showed that several adsorptive sites were competing for adsorption of Zn^{2+} .

The intra particle diffusion adequately gave a good fitting with R^2 at 0.9567. The boundary layer thickness (C) showed a small layered thickness at 0.1825, and K_{id} known

as the intra-particle rate constant was 0.0182. Both were small values < 1 and affected the rate constant. Therefore, the intra-particle diffusion was not the rate-determining step among the adsorption processes and the graph did not pass through the origin having intercept $C > 0 < 1$. Thus, it was affected by some other adsorptive processes in the system as similarly shown by $1/\beta$ in Elovich, K_1 in pseudo 2nd order and H in pseudo 1st order. Also, our study provided a better fitting of Elovich function and intra-particle diffusion compared to [29].

CONCLUSIONS

The neutral pH 7 contributed to the maximum removal of Zn^{2+} by GO. Langmuir isotherm showed that the reaction was favourable while the Freundlich showed that the energy of adsorption was small and hence driving a slow endothermic process which correlated with the results from the Dubinin Radushkevich. Temkin showed that there was a weak binding interaction and hence a physical adsorption process in the system. The pseudo 2nd order showed faster reaction kinetics compared to pseudo 1st order reaction as shown by its absolute slope of 2.268 and an intercept of 34.62. Elovich function showed that the adsorption process was non spontaneous and intra-particle diffusion was not the rate-determining step. In conclusion, all the eight adsorptive functions showed the proficiency of graphene oxide in the removal of zinc(II) ions from aqueous solution. Moreover, the results were largely affected/dependent on method of synthesis as pointed out by [5]. Finally, the research work will contribute to the potential functionalization of Zn^{2+} and graphene nano-composite materials for various applications [37,33]

ACKNOWLEDGEMENTS

The authors acknowledge the Department of Chemistry, School of Physical Sciences, FUTO Owerri, Nigeria for their involvement and contribution during this research.

REFERENCES

- [1] Ankur, G.; Tamilselvan, S.; Sudipta, S., Recent

- development in 2D materials beyond graphene. *Prog. Mater. Sci.* **2015**, *73*, 44-126. DOI: 10.1016/j.pmatsci.2015.02.002.
- [2] Velram, B.; Dongyan, L.; Krishnan, J.; Manfred, S.; Debes, B., Improvements in electronic structure and properties of graphene derivatives. *Adv. Mater. Lett.* **2016**, *7*, 421-429. DOI: 10.5185/amlett.2016.6123.
- [3] Nkwoada, A.; Amakom, C.; Oguzie, E., The role and economics of nano-graphene functionalization in Oil industry improvement. *Asian J. Phy. Chem. Sci.* **2018**, *5*, 1-19. DOI: 9734/AJOPACS/2018/39683.
- [4] Minh-Hai, T.; Cheol-Soo, Y.; Sunhye, Y.; Ick-Jun, K.; Hae, K., Influence of graphite size on the synthesis and reduction of graphite oxides. *Curr Appl. Phys.* **2014**, *14*, S74-S79.
- [5] Dreyer, D.; Park, S.; Bielawski, C.; Ruoff, R., The chemistry of graphene oxide. *Chem. Soc. Rev.* **2010**, *39*, 228-240. DOI: 10.1039/b917103g.
- [6] Cooper, D. R.; D'Anjou, B.; Ghattamaneni, N.; Harack, B.; Hilke, M.; Horth, A.; Majlis, N.; Massicotte, M.; Vandsburger, L.; Whiteway, E.; Yu, V., Experimental review of graphene. *ISRN Condens. Matter Phys.* **2012**, Article ID 501686, 1-56. DOI: 10.5402/2012/501686.
- [7] Navnath, B.; Sneha, R., Graphene and its applications: A survey. *Asian J. Sci. Technol.* **2016**, *7*, 2596-2599.
- [8] Fen, L.; Xue, J.; Jijun, Z.; Shengbai, Z., Graphene oxide: A promising nanomaterial for energy and environmental applications. *Nano Energy.* **2015**, *16*, 488-515. DOI: 10.1016/j.nanoen.2015.07.014.
- [9] Hakimi, M.; Alimard, P., Graphene: Synthesis and applications in biotechnology: A review. *World Appl. Prog.* **2012**, *2*, 377-388. DOI: 10.3109/21691401.2014.927880.
- [10] Shamaila, S.; Sajjad, A.; Iqbal, A., Modifications in development of graphene oxide synthetic routes. *Chem. Eng. J.* **2016**, *294*, 458-477. DOI: 10.1016/j.cej.2016.02.109.
- [11] Tien-Tsai, W.; Jyh-Ming, T., Preparation and characteristics of graphene oxide and its thin films. *Surf. Coat. Technol.* **2013**, *231*, 487-491. DOI: 10.1016/j.surfcoat.2012.05.066.
- [12] Paulchamy, B.; Arthi, G.; Lignesh, B., Simple approach to stepwise synthesis of graphene oxide Nanomaterial. *J. Nanomed. Nanotechnol.* **2015**, *6*. DOI: 10.4172/2157-7439.1000253.
- [13] Botas, C.; Alvarez, P.; Blanco, P.; Granda, M.; Blanco, C.; Santamari, R.; Romasanta, J. L.; Verdejo, R.; Lopez-Manchado, M. A.; Menendez, R., Graphene materials with different structures prepared from the same graphite by the hummers and brodie methods. *Carbon.* **2013**, *65*, 156-164. DOI: 10.1016/j.carbon.2013.08.009.
- [14] Shahriary, L.; Athwale, A., Graphene oxide synthesized by using modified hummers approach. *Int. J. Renew. Energy Environ. Eng.* **2014**, *2*.
- [15] Jianguo, S.; Xinzhi, W.; Chang-Tang, C., Preparation and characterization of graphene oxide. *J. Nano. Mater.* **2014**, Article ID 276143. DOI: 10.1155/2014/276143.
- [16] Miyeon, L.; Jihoon, L.; Sung, Y.; Byunggak, M.; Bongsoo, K.; Insik, I., Production of graphene oxide from pitch-based carbon fibre. *Sci. Reports.* **2015**, *5*. DOI: 10.1038/srep11707.
- [17] Folke, J.; Karlheinz, G.; Rolf, M., Scale-up and purification of graphite oxide as intermediates for functionalized graphene. *Carbon.* **2014**, *75*, 432-442. DOI: 10.1016/j.carbon.2014.04.022.
- [18] Kosynkin, D.; Higginbotham, A.; Sinitskii, A.; Lomeda, J.; Dimiev, A.; Price, K.; Tour, Longitudinal unzipping of carbon nanotubes to form graphene nanoribbons. *Nature.* **2009**, *458*, 872-876.
- [19] Yuta, N., Improved synthesis of graphene oxide and its Application to Nanocomposites. Intellectual Property and Enterprise: OKAYAMA University e-bulletin. 2013, 3.
- [20] Marcano, D.; Kosynkin, D.; Berlin, J.; Sinitskii, A.; Sun, Z.; Slesarev, A.; Tour, J., Improved synthesis of graphene oxide. *ACS Nano.* **2010**, *4*, 4806-484. DOI: 10.1021/nn1006368.
- [21] Higginbotham, A.; Kosynkin, D.; Sinitskii, A.; Sun, Z.; Tour, J., Lower-defect graphene oxide nanoribbons from multi-walled carbon nanotubes. *ACS Nano.* **2010**, *4*, 2059-2069. DOI: 10.1021/nn100118m.
- [22] Wang, X.; Guo, Y.; Li, Y.; Han, M.; Zhao, J.; Cheng, X., Nanomaterials as sorbents to remove heavy metal ions in wastewater treatment. *J. Environ. Anal.*

- Toxicolo.* **2012**, *2*. DOI: 10.4172/2161-0525.1000154.
- [23] Kyzas, G.; Deliyanni, E.; Matis, K., Graphene oxide and its application as an adsorbent for wastewater treatment. *J. Chem. Technol. Biotechnol.* **2014**, *89*, 196-205. DOI: 10.1002/jctb.4220.
- [24] Bin, H.; Zuowei, X., Determination of trace/ultra trace rare earth elements in environmental samples by ICP-MS after magnetic solid phase extraction with Fe₃O₄@SiO₂@polyaniline graphene oxide composite. *Talanta.* **2014**, *119*, 458-466. DOI: 10.1016/j.talanta.2013.11.027.
- [25] Hui, H.; Ting, C.; Xiuyu, L.; Houyi, M., Ultrasensitive and simultaneous detection of heavy metal ions based on three-dimensional graphene-carbon nanotubes hybrid electrode materials. *Anal. Chimica Acta.* **2014**, *852*, 45-54. DOI: 10.1016/j.aca.2014.09.010.
- [26] Najafi, F., Removal of zinc(II) ion by graphene oxide (GO) and functionalized graphene oxide-glycine (GO-G) as adsorbents from aqueous solution: kinetics studies. *Int. Nano Lett.* **2015**, *5*, 171-178. DOI: 10.1007/s40089-015-0151-x.
- [27] Chungsyng, L.; Huantsung, C., Adsorption of zinc(II) from water with purified carbon nanotubes. *Chem. Eng. Sci.* **2006**, *61*, 1138-1145. DOI: 10.1016/j.ces.2005.08.007.
- [28] Nkwoada, A.; Okoli, K.; Ekeanyanwu, I., Novel Kinetic modelling and optimization for adsorption of Zn²⁺ over graphene oxide. *J. Appl. Chem. Sci. Int.* **2016**, *7*, 64-70.
- [29] Hou, W.; Xingzhong, Y.; Yan, W.; Huajun, H.; Guangming, Z.; Yan, L.; Xueli, W.; Ningbo, L.; Yu, Q., Adsorption characteristics and behaviors of Graphene oxide for Zn(II) removal from aqueous solution. *Appl. Surf. Sci.* **2013**, *279*, 432-440. DOI: 10.1016/j.apsusc.2013.04.133.
- [30] Dada, A.; Olalekan, A.; Olatunya, A.; Dada, O., Langmuir, freundlich, temkin and dubinin-radushkevich isotherms studies of equilibrium sorption of Zn²⁺ unto phosphoric acid modified rice husk. *IOSR J. Appl. Chem.* **2012**, *3*, 38-45. DOI: 10.9790/5736-0313845.
- [31] Abuh, M.; Akpomie, G.; Nwagbara, N.; Abia-Bassey, N.; Akpe, D.; Ape.; Ayabie, B., Kinetic rate equations application on the removal of copper(II) and zinc(II) by unmodified lignocellulosic fibrous layer of palm tree trunk-single component system studies. *Int. J. Basic Appl. Sci.* **2013**, *3*, 800-809.
- [32] Sharma, R.; Chadha, N.; Saini, P., Determination of defect density, crystallite size and number of graphene layers in graphene analogues using X-ray diffraction and Raman spectroscopy. *Indian J. Pure Appl. Phys.* **2017**, *55*, 625-629.
- [33] Sohail, M.; Saleem, M.; Ullah, S.; Saeed, N.; Afridi, A.; Khan, M., Modified and improved hummers synthesis of graphene oxide for capacitors applications. *Mod. Electron. Mater.* **2017**, *3*, DOI: 10.1016/j.moem.2017.07.002.
- [34] Imtithal, S.; Ahmad, K.; Hanafy, H., Removal of heavy metals using nanostructured graphite oxide, silica nanoparticles and silica/graphite oxide composite. In Elsevier (Ed.). The Int. Conf. Technol. Mater. Renew Energy, Environ. Sustain. *TMREES14.* **2014**, *50*, 130-138. DOI: 10.1016/j.egypro.2014.06.016.
- [35] Somphob, T.; Thanyada, R.; Oraphan, S.; Supot, H., A computational study of adsorption of divalent metal ions on graphene oxide. *Songklanakarin J. Sci. Technol.* **2017**, *39*, 773-778. DOI: 10.14456/sjst-psu.2017.94.
- [36] Sitko, R.; Turek, E.; Zawisz, B.; Malick, E.; Talik, E.; Heimann, J.; Wrzalik, R., Adsorption of divalent metal ions from aqueous solutions using graphene oxide. *Dalton Trans.* **2013**, *42*, 5682-5689. DOI: 10.1039/c3dt33097d.
- [37] Wei, L., Preparation of a zinc oxide-reduced graphene oxide nanocomposite for the determination of cadmium(II), lead(II), copper(II), and mercury(II) in water. *Int. J. Electrochem. Sci.* **2017**, *12*, 5392-5403. DOI: 10.20964/2017.06.06.